Science of the Total Environment 956 (2024) 177358

Contents lists available at ScienceDirect

Science of the Total Environment

journal homepage: www.elsevier.com/locate/scitotenv

Probing ozone effects on European hornbeam (*Carpinus betulus* L. and *Ostrya carpinifolia* Scop.) leaf water content through THz imaging and dynamic stomatal response

Mario Pagano [a,1], Yasutomo Hoshika [a,b,1], Fulvia Gennari [d,*], Jacopo Manzini [a,c], Elena Marra [a], Andrea Viviano [a,c], Elena Paoletti [a,b], Sharmin Sultana [d], Alessandro Tredicucci [d,e,f], Alessandra Toncelli [d,e,f,g]

[a] Institute of Research on Terrestrial Ecosystems (IRET), National Research Council (CNR), Via Madonna del Piano 10, 50019 Sesto Fiorentino, Italy
[b] NBFC, National Biodiversity Future Center, Palermo 90133, Italy
[c] DAGRI, University of Florence, Piazzale delle Cascine 18, 50144 Firenze, Italy
[d] Dipartimento di Fisica "E. Fermi", Università di Pisa, Largo B. Pontecorvo 3, 56127 Pisa, Italy
[e] Centro per l'Integrazione della Strumentazione dell'Università di Pisa (CISUP), Lungarno Pacinotti 43/44, 56126 Pisa, Italy
[f] Istituto Nanoscienze – CNR, Piazza S. Silvestro 12, 56127 Pisa, Italy
[g] Istituto Nazionale di Fisica Nucleare, Sezione di Pisa, Largo B. Pontecorvo 3, 56127 Pisa, Italy

HIGHLIGHTS

- O_3 effects on photosynthesis and leaf water status in two Hornbeam species
- THz imaging and dynamic stomatal response analysis for pollution monitoring
- THz imaging detected dry spots on leaves better than visible images.
- O_3 promoted stomatal sluggishness mostly in *C. betulus* than in *O. carpinifolia*.
- Comprehensive understanding of Hornbeam adaptive strategies to O_3 fumigation.

GRAPHICAL ABSTRACT

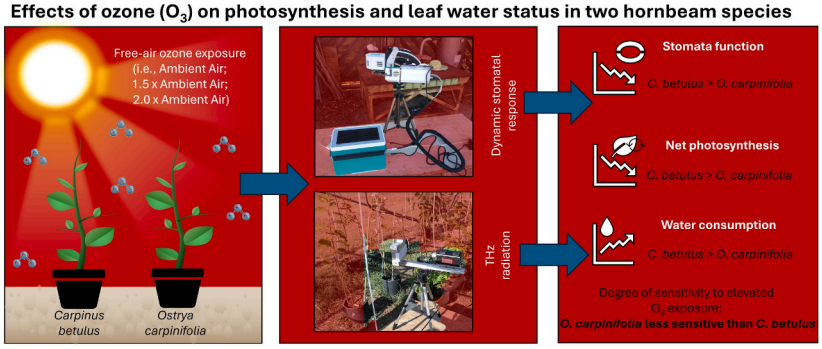

ARTICLE INFO

Editor: Jay Gan

Keywords:
Hornbeam
Terahertz
Imaging data
Stomatal conductance
Ozone (O_3) induced

ABSTRACT

We investigated the impact of ozone exposure on Hornbeam using a novel dual approach based on Terahertz (THz) imaging in a free-air ozone exposure experiment (three ozone levels: ambient; 1.5 times ambient; twice ambient). The research aims at unraveling the physiological responses induced by elevated ozone levels on water dynamics. THz imaging unveiled dynamic changes in leaf water content, providing a non-invasive approach to leaf water monitoring. Leaf gas exchange measurements assessed stomatal responses to light variation. Our findings showcase a compelling correlation between elevated ozone levels and reduction in photosynthetic rate and impairment of stomatal function, i.e. "stomatal sluggishness", indicative of nuanced regulatory mechanism.

* Corresponding author.
E-mail address: fulvia.gennari@phd.unipi.it (F. Gennari).
[1] These authors contributed equally to the work.

https://doi.org/10.1016/j.scitotenv.2024.177358
Received 5 September 2024; Received in revised form 29 October 2024; Accepted 31 October 2024
Available online 7 November 2024

Stomatal sluggishness was particularly evident in *Carpinus betulus* (CB) compared to *Ostrya carpinifolia* (OC) and was linked to reduction in photosynthetic capacity. THz-based imaging techniques confirmed this result indicating a negative effect of O_3 on leaf-level total water content. In addition, spatial analysis of leaf water status using these techniques also highlighted that the negative effect of O_3 on water status was progressing even in less sensitive OC plants though visible foliar injury was not detected. In fact, OC showed a relative dry area of 1.6 ± 1.6 % in the control group and 3.8 ± 1.3 % under high ozone levels. THz-based imaging techniques provided a deep understanding of O_3 behavior in plants and may be recommended for precision biosensing in the early detection of O_3-induced damage. The integration of THz imaging and physiological analysis resulted in comprehensive understanding of Hornbeam acclimation response to ozone exposure.

1. Introduction

In the biosphere, anthropogenic trace gas emissions and absorptions impact atmospheric chemistry and may have unforeseen consequences including climate change, air pollution, and nitrogen and carbon cycles imbalance (IPCC, 2013). One of the most significant trace gasses in the atmosphere is tropospheric ozone (O_3), which enters plants through stomata causing damage to physiological processes (Grulke and Heath, 2020; Agrawal et al., 2021). Ozone is a phytotoxic product resulting from photoreactions of O_3 precursors like volatile organic compounds (VOC) — both biogenic and anthropogenic — as well as NO, and NO_2 (Mochizuki et al., 2020), and its production could be accelerated by global warming (Wada et al., 2023). Many studies claimed that high O_3 concentrations raise the risk of crop yield reductions, stunted growth in forests, and other health hazards to plants (De Marco et al., 2022; Feng et al., 2022). Reduced activities of biochemical parameters such as carboxylation efficiency are among the most common effects of O_3 on plant photosynthesis, in addition to lower stomatal conductance that limits CO_2 uptake (Kitao et al., 2009; Hoshika et al., 2020). In addition, O_3 may impair the regulation of water loss by inducing less responsive stomatal response, i.e. 'stomatal sluggishness' (Paoletti, 2005; Paoletti and Grulke, 2010; Hoshika et al., 2012, 2019). A lower stomatal sensitivity to environmental stimuli was reported according to sap flow measurements in a southern Appalachian Forest in the U.S., suggesting that the stomatal sluggishness due to O_3 exposure reduced water use efficiency and increased transpiration rates, even during drought stress (McLaughlin et al., 2007; Sun et al., 2012). A modeling study claimed that the current O_3 levels (~40 ppb) potentially reduce the water use efficiency of deciduous forests by 7 % in the Northern Hemisphere due to O_3-induced stomatal sluggishness (Hoshika et al., 2015). However, our knowledge is still scarce about how the stomatal sluggishness affects the water status at the leaf level after O_3 exposure. Over the years, many studies have been carried out for different species to non-destructively look at the plant acute reaction to O_3 including the intricate physiological responses induced by elevated O_3 levels (Ansari et al., 2023; Peng et al., 2020, Endo and Omasa, 2007; VanLoocke et al., 2012; Cotrozzi et al., 2020).

One of the most sensitive technologies for the non-destructive assessment of plant stress are THz spectroscopy, the infrared canopy temperature method, and THz imaging (Zhang et al., 2023). THz radiation has high penetration and sensitivity to the absorption of water (Rawson and Sunil, 2022). THz radiation imaging and spectroscopy have been used as noninvasive instruments for estimating the leaf water status, which refers to the hydration level of a leaf, (Gente and Koch, 2015; Baldacci et al., 2017; Pagano et al., 2019), under various conditions, for instance drought stress (Born et al., 2014;), circadian rhythm change (Torres et al., 2016), low temperature stress, and dehydration kinetics (Castro-Camus et al., 2013). Hence, THz spectroscopy is expected to reveal O_3 stress related changes in plants, as it depicts the transformations and spatial variations in the leaf water status associated with the physiological responses induced by O_3 exposure. To the best of our knowledge, no studies have been conducted to unravel the intricate physiological responses induced by elevated O_3 using THz imaging. This research attempts to explore the feasibility of using THz imaging to monitor the O_3-induced stomatal sluggishness effects on leaf water status using two common European Hornbeam species (namely, *Carpinus betulus* L. and *Ostrya carpinifolia* Scop.). Studies regarding the impact of O_3 tolerance of mature European hornbeam trees are currently scarce. Günthardt-Goerg et al. (1999) examined the O_3-induced visible foliar injury for *C. betulus*, while Marzuoli et al. (2018) conducted an open-top chamber experiment on *C. betulus* suggesting that their sensitivity to O_3 varied with nutrient availability. On the other hand, there is no study for testing the O_3 impacts on *O. carpinifolia*. In this study, a comprehensive understanding of Hornbeam photosynthetic and water use responses to O_3 is warranted by the combination of THz imaging and stomatal conductance analysis.

This study aims at untangling the complex interactions between O_3 exposure, water dynamics, and stomatal activities of the two Hornbeam species. We postulate that *O. carpinifolia* may be more tolerant to O_3 stress than *C. betulus* due to different leaf morphological traits such as presence of trichomes and cuticle thickness and a relatively high leaf mass per area (LMA) (Uzunova, 1999; Bastias et al., 2020), resulting from its preference to warmer and drier environment (Pasta et al., 2016; Sikkema et al., 2016). Ozone sensitivity may be related to drought tolerance (Hoshika et al., 2020) because plants adapted to arid environments may have developed mechanisms to cope with drought stress in association with elevated detoxification capacity and morphological adaptation, which also play an important role for physical and biochemical defense against O_3 stress (Manes et al., 1998; Marchica and Pellegrini, 2023).

2. Materials and methods

2.1. Experimental site and plant material

The experiment was conducted on two European hornbeam species namely: *Carpinus betulus* L. (CB) and *Ostrya carpinifolia* Scop. (OC). Two-years-old seedlings were obtained from a tree nursery (Vivai Guagno, Comacchio, Italy). In May 2023, plants were transported to the CNR experimental garden and transplanted into plastic pots (volume 10 L). The substrate was composed of peat, pumice and field soil (ratio 1:1:1). The plants were maintained under field conditions until the beginning of the O_3 treatments. From 29th May to 31st October 2023, they were exposed to three O_3 levels, namely ambient (AA), 1.5 times ambient O_3 (1.5 × AA), and twice ambient O_3 (2.0 × AA), at the O_3 Free-Air Controlled Exposure (FACE) facility located in Sesto Fiorentino, Italy (43°48′49" N, 11°12′01″ E, 55 m a.s.l.), as detailed in Paoletti et al. (2017). The values of AOT40 (Accumulated O_3 exposure over the Threshold of 40 ppb) were 16.2 ppm•h in AA, 40.1 ppm•h in 1.5 × AA, 78.2 ppm•h in 2.0 × AA. Three plants for each species were assigned in each replicated plot ($n = 3$ plots) in each O_3 treatment (in total 27 plants for each species). Plants were watered every day (mean volumetric soil water content = 0.264 $m^3\ m^{-3}$, as 89 % of field capacity, Paoletti et al., 2017) to avoid any water stress for hornbeam plants (Gerosa et al., 2022).

2.2. Measurements of steady-state and dynamic gas exchange

Leaf gas exchange was measured in fully-expanded sun-exposed leaves (1 to 2 plants for each replicated plot for each O_3 treatment for each species) with a portable infra-red gas analyzer (Model 6800, Li-Cor instruments, Lincoln, NE, USA) under the control condition of Li-Cor cuvette (leaf temperature: 25 °C, relative humidity: 50 %, ambient CO_2 concentration: 410 μmol mol^{-1}). After net photosynthetic rate (A) and stomatal conductance (g_s) reached equilibrium at a constant light [Photosynthetic Active Radiation (PAR): 1500 μmol m^{-2} s^{-1}], the light intensity was changed to a low light condition (PAR = 100 μmol m^{-2} s^{-1}) until a new equilibrium of A and g_s was found, then back again to a high light condition (PAR = 1500 μmol m^{-2} s^{-1}), according to the methodology described in Paoletti (2005) and Hoshika et al. (2012). Leaf gas exchange parameters were recorded at 30 s intervals. As a result, the steady-state values of leaf gas exchange, and the intrinsic water use efficiency (defined as A divided by g_s) were calculated under both high (A1500, g_s1500) and low light conditions (A100 and g_s100). In addition, following the method by Gerardin et al. (2018) and Durand et al. (2019), we fitted a sigmoid model to the dynamic response of g_s (Vialet-Chabrand et al., 2013):

$$g_s = r0 + (G - r0)^{*} exp\left(- exp\left(\frac{\lambda - t}{\tau}\right)\right)$$

where r0 represents the initial g_s value at the steady state, G denotes the final g_s value in response to the change of light intensity. λ is the time required to reach the inflection point of the curve following the light change. τ refers to the overall response time. According to this model, the maximum slope (SL_{max}) as an indicator of the stomatal response speed, which can be calculated as:

$$SL_{\max} = (l/\tau)^{*}(G - r0)/e$$

where e is the Euler's number (≈ 2.718). SL_{max} was calculated for both stomatal opening (SL_{max_open}) and closure (SL_{max_close}) for the change of light intensity. We also calculated the following parameters according to Freitas et al. (2023): Δg_s: amplitude of g_s when changing light intensity; $T90_{open}$ and $T90_{close}$: time to reach 90 % of the maximum change in stomatal opening and closure, respectively.

2.3. Imaging setup and analysis

2.3.1. Visible imaging

Visible (RGB) images of the leaves were obtained using an EOS 1100D camera (Canon, Tokyo, Japan) with EFS 18–55 mm 0.25 m/0.8 ft. macro-objective (Canon, Japan). After capturing the leaf shape on camera, the leaf area (L_A) was measured using ImageJ 1.50i software (National Institutes of Health, Bethesda, MD, USA). L_A processing consisted of the following steps: Open image, analyze, set scale, and select polygon (as a tool for outlining the leaf perimeter).

2.3.2. Terahertz imaging

The terahertz (THz) imaging system was composed of an impact avalanche transit time (IMPATT) diode source (IMPATT-100-H/F, Terasense, San Jose, USA) with a nominal output power of 30 mW and an output frequency of 140 GHz. Additionally, a THz camera (T15/32/32, Terasense, San Jose, USA) was utilized, comprising a square matrix of sensors (32 × 32 pixels, sensor size 48 × 48 mm). This device has already been tested on various biological samples and can record both single images and continuous videos (Di Girolamo et al., 2020). The diode source and the THz camera were located approximately 40 cm apart, optimized to achieve the most uniform illumination in the area occupied by the leaf on the detector. Moreover, the exposure time of the image was fine-tuned to prevent saturation of the pixel signal. The gamma correction was consistently set to the value corresponding to linear response of the pixels, ensuring better reproducibility of results across repeated acquisitions. Although non necessary for THz imaging, the leaves were detached from the plant for the subsequent gravimetric measurements, and immediately the detached leaves were gently pressed on the sensor with a Teflon mask one by one to acquire images of the outstretched leaves.

2.3.3. Image analysis

The analysis of THz images and subsequent statistical processing were conducted using Matlab software (version R2022b). For the gravimetric calibration, the leaf area was automatically identified and cropped from the whole image, then the average signal intensity within the leaf was determined for both the sample image and the background image acquired without any leaf on the sensor in the same area. The mean attenuation in the sample was then computed as the ratio between the two average intensities, as expressed by the following formula:

$$A_{THz} = log\frac{\sum_{i,j} I_{bkg_{i,j}}}{\sum_{i,j} I_{tr_{i,j}}}$$

where I_{bkg} was the background intensity, I_{tr} was the sample intensity, and the i and j indexes run over all the pixels in the leaf cropped area. Since the THz signal is expected to be linearly correlated with the leaf water content, possible water distribution inhomogeneities are expected to appear as partially transmitting spots in the THz image. To identify these possible dry spots, we set up an automatic procedure to find pixels with an intensity higher than a certain threshold value set at 20 % lower than the background value. This value was chosen as a tradeoff to consider the right parts of the leaves and not the background noise.

Only spots larger than 8 contiguous pixels were taken into account. The total area of the identified dry spots was taken as a measure of the dry parts of the leaves. Visible images were analyzed using ImageJ software. With this software, we manually identified all the brown and black spots within the leaf and calculated their total area. For the analysis of the dry spots of the leaves, the portion of each leaf close to the perimeter was excluded both in the visible and in the THz case. Excluding the perimeter is due to the fact that the central part of the leaf is thicker and richer in water, therefore, it better interacts with the THz radiation and gives a better sensitivity. It may be worth noting that with this method we could only analyze the leaves that were smaller than our detector area, therefore, this analysis has been carried out on 11 leaves per species per treatment.

2.4. Water mass assessment and leaf traits

For all species and treatments (AA, 1.5 × AA, 2.0 × AA), leaf samples (15 leaves randomly sampled for each treatment) were weighed on an analytical balance (Sartorius, Germany) to assess the fresh weight (F_W). Subsequently, the same leaves were oven dried for 5 days at 70 °C until constant weight in order to determine their dry weight (D_W). Finally, the absolute leaf water mass (W_m) was calculated as the difference between the fresh and dry mass. In agreement with Pagano and Baldacci (Pagano et al., 2019; Baldacci et al., 2017), the linear relationship between the leaf water content of the samples and the THz attenuation (A_{THz}) multiplied by the leaf area (L_A) was then checked. The values of LMA were calculated as the ratio of D_W to L_A.

The stomatal density was measured using the SUMP method (Koike et al., 1998). This technique involves creating a replica of the abaxial leaf surface with a celluloid sheet (Universal Micro-printing, SUMP, Tokyo, Japan). Stomata were counted at 5 to 7 randomly selected locations within the intercostal fields (3 leaves per plant, 1 to 2 plants per each plot per treatment in both species), each with an area of 0.4 mm^2, under a light microscope.

2.5. Statistics

A well-replicated split-plot design was implemented, consisting of

three replicated plots. The whole-plot factor was the O_3 levels, while the two hornbeam species were randomly assigned to six pots within each plot (three pots per species). Normal distribution was assessed using the Shapiro-Wilk test. As the data followed a normal distribution, we conducted a full-factorial split-plot two-way analysis of variance (ANOVA) for the leaf traits (LMA, stomatal density) and leaf gas exchange parameters, with O_3 and species as fixed factors, and the plot treated as a random factor nested within the O_3 levels.

The THz calibration measurements were conducted on all the theses, utilizing a total of 45 leaves. On the contrary, comparisons among the different treatments were based on 25 replicated leaves per treatment per species. To estimate absolute leaf water mass, the calibration model of THz acquisition was established by a linear regression analysis for each hornbeam species. As the calibration model was dependent on species, statistical difference for THz acquisition among O_3 treatments for each species was determined using a split-plot one-way ANOVA test. Results were considered significant at $p < 0.05$. The statistical analysis was conducted using Microsoft Excel (Microsoft) and GraphPad Prism v. 10 Demo (GraphPad software).

3. Results

3.1. Leaf mass per area and stomatal density

Higher LMA values were found in OC compared to CB plants. On the other hand, stomatal density was higher in CB than OC plants. There was no significant difference in both parameters among the O_3 treatments (Table 1).

3.2. Steady-state and dynamic response of leaf gas exchange to light intensity

Twice ambient O_3 concentrations decreased $A1500$ and $A100$ especially in CB plants (Table 2). However, there was no significant effect of O_3 on steady-state g_s values in both species. The negative effect of O_3 on iWUE was observed in CB leaves exposed to 2.0 × AA whereas such a reduction was not found in OC as confirmed by the interaction of O_3 and species.

For the dynamic response when changing the light intensity from high to low, g_s showed a gradual decrease in AA, while we found a sharp decrease in values of A regardless of the different plant species (Fig. 1). On the other hand, when the light intensity was changed again to the high values, both leaf gas exchange parameters showed a gradual increase. There was no statistical significance between O_3 treatments for most of the parameters of dynamic stomatal response (Table 3).

Table 1
Leaf mass per unit area (LMA) and stomatal density for *Carpinus betulus* (CB) and *Ostrya carpinifolia* (OC) grown under three levels of ozone. The values (mean ± S.E.) were calculated based on the values of the measured individuals ($n = 8$ to 9 plants [2 to 3 plants per each plot per each O_3 treatment] for LMA and $n = 3$ to 4 plants [1 to 2 plants per each plot per each O_3 treatment] for stomatal density). Asterisks show the significance of ANOVA: ***$p < 0.001$, ns: not significant.

Species	Ozone	LMA ($g\ m^{-2}$)	Stomatal density (mm^{-2})
CB	AA	93.8 ± 3.3	93.1 ± 8.9
	1.5 × AA	90.0 ± 3.5	93.7 ± 8.3
	2.0 × AA	100.5 ± 5.1	121.8 ± 12.5
OC	AA	106.1 ± 6.4	57.0 ± 1.5
	1.5 × AA	103.0 ± 5.0	58.4 ± 6.1
	2.0 × AA	119.8 ± 6.2	65.4 ± 5.6
ANOVA results			
	O_3	ns	ns
	Species	***	***
	O_3 × Species	ns	ns

However, the effect of O_3 was significant for SL_{max_close}, which shows the rate of closing response of stomata with decreasing light intensities. The negative effect of O_3 on stomatal closing was more evident in CB (CB: −56 % in 1.5 × AA, −79 % in 2.0 × AA; OC: −28 % in 1.5 × AA, −25 % in 2.0 × AA). In fact, some CB leaves after 2.0 × AA O_3 exposure showed almost no response of g_s with changing light intensity.

3.3. THz image analysis

The model exhibited an R-squared value of 0.85 and 0.76 for CB and OC, respectively, regardless of the O_3 exposure level (Fig. 2A, B). Given this established linear correlation, we used the A_{THz} x L_A data as a measurement directly proportional to the leaf water mass. Statistical analysis of the A_{THz} x L_A data on 25 leaves per each treatment per species showed a decreasing trend of the water mass with increasing ozone exposure, although statistical ANOVA results indicated a significant decrease in water mass only between the AA and 2.0 × AA treatments in both species (Fig. 2C, D). In fact, both CB and OC 2.0 × AA showed a significant decrease of −43.8 % and −49.1 %, respectively, compared to their respective control groups. THz and visible images were also used for identifying possible dry spots in the internal area of the leaves. An example of typical images of leaves of OC is shown in the Supplementary Information. The total dry area calculated from the dry spots was compared in the two spectral ranges. While visible analysis both in CB and OC indicated an area compatible with null result (0.4 ± 0.8 % and 0.4 ± 0.6 %, respectively), the THz image analysis shows 2.4 ± 1.2 % of CB and 3.8 ± 1.3 % of OC relative dry area (Fig. 3). This result suggests that THz imaging can be used in the early detection of ozone damage. The relative dry area in AA and in 2.0 × AA nearly overlapped each other in CB (Fig. 4). On the other hand, OC presented a sharp separation between the two distributions of the populations. More in detail, CB had a relative dry area of 2.8 ± 1.6 % and 2.4 ± 1.2 % in AA and in 2.0 × AA, respectively, while OC showed 1.6 ± 1.6 % and 3.8 ± 1.3 % relative dry area in AA and in 2.0 × AA, respectively.

4. Discussion

The dynamic response of A and g_s with changing environmental factors has been widely investigated in ecology, plant physiology, global climate change biology, and modeling research (Kattge et al., 2009). In a natural environment, there is a temporal change in the light intensity received on leaves and thus leaves utilize the fluctuating PAR, which strongly impacts their ability to gain carbon and water loss through stomata (Tinoco-Ojanguren and Pearcy, 1993; Tomimatsu and Tang, 2012; Agathokleous et al., 2023). In the present study, measurements of dynamic stomatal response revealed that O_3 exposure decreased the closing speed of stomata with decreasing light intensity rather than its opening speed. Ozone exposure led to a significant decline in the steady-state photosynthesis, consistent with the findings from previous meta-analysis (Wittig et al., 2007; Li et al., 2017), especially in CB, whereas steady-state g_s was not significantly changed by O_3 in either high or low light conditions. Similar findings were reported in *Acer saccharum* leaves where O_3 exposure significantly decreased photosynthetic rate even though g_s remained high (Tjoelker et al., 1995). Although g_s is typically tightly correlated with photosynthesis (Larcher, 2003), a decoupling of g_s from A after O_3 exposure was often observed (Lombardozzi et al., 2012; Hoshika et al., 2020, 2022). As a result, a decrease in Intrinsic water-use efficiency (iWUE) was highlighted in 2.0 × AA O_3-exposed CB leaves, potentially indicating an impairment of efficient stomatal control to water loss for tree growth under O_3 polluted environments. A negative effect of O_3 on leaf gas exchange was highlighted in CB rather than OC plants. A remaining opened stoma might contribute to promote CO_2 diffusion into a leaf resulting in some positive effects on photosynthetic carbon gain as a compensatory response (Watanabe et al., 2014). However, it should be noted that, during a prolonged O_3 exposure, the sluggish stomatal closing response observed under 2.0 × AA may have

Table 2
Effects of ozone exposure on steady-state leaf gas exchange in *Carpinus betulus* (CB) and *Ostrya carpinifolia* (OC) grown under three levels of ozone. The values (mean ± S.E.) were calculated based on the values of the measured individuals (n = 4 to 6 plants [1 to 2 plants per each plot per each O_3 treatment]). Asterisks show the significance of ANOVA: ***$p < 0.001$, **$p < 0.01$, *$p < 0.05$, ns: not significant. When finding the interaction of O_3 and species, a Tukey post-hoc test was applied. Different letters show significant differences among means ($p < 0.05$). NV: Herein, ambient air, AA; 1.5 times ambient ozone concentration, 1.5 × AA; twice ambient ozone concentration, 2.0 × AA). A1500 and A100: net photosynthesis at 1500 and 100 μmol m^{-2} s^{-1} PAR, respectively; g_s1500 and g_s100: stomatal conductance at 1500 and 100 μmol m^{-2} s^{-1} PAR, respectively; iWUE1500 and iWUE100: intrinsic water use efficiency at 1500 and 100 μmol m^{-2} s^{-1} PAR, respectively.

Species	Ozone	A1500	A100	g_s1500	g_s100	iWUE1500	iWUE100
		(μmol m^{-2} s^{-1})	(μmol m^{-2} s^{-1})	(mol m^{-2} s^{-1})	(mol m^{-2} s^{-1})	(μmol mol^{-1})	(μmol mol^{-1})
CB	AA	7.5 ± 1.2	2.9 ± 0.3	0.118 ± 0.028	0.059 ± 0.020	68.2 ± 3.9 a	60.3 ± 2.4 a
	1.5 × AA	6.7 ± 0.8	2.6 ± 0.1	0.116 ± 0.019	0.045 ± 0.002	63.5 ± 4.2 a	57.5 ± 1.5 a
	2.0 × AA	3.0 ± 0.7	1.6 ± 0.1	0.072 ± 0.012	0.062 ± 0.008	41.3 ± 4.6 b	26.7 ± 3.4 b
OC	AA	8.2 ± 0.7	3.3 ± 0.4	0.103 ± 0.013	0.052 ± 0.010	82.2 ± 4.4 a	66.2 ± 5.4 a
	1.5 × AA	6.7 ± 0.5	2.2 ± 0.1	0.115 ± 0.019	0.047 ± 0.005	62.7 ± 5.3 a	50.0 ± 6.7 a
	2.0 × AA	6.6 ± 0.9	2.1 ± 0.3	0.097 ± 0.013	0.039 ± 0.007	69.0 ± 6.3 a	56.8 ± 5.1 a
ANOVA results							
	O_3	*	*	ns	ns	*	**
	Species	*	ns	ns	ns	**	***
	O_3 × Species	ns	ns	ns	ns	**	***

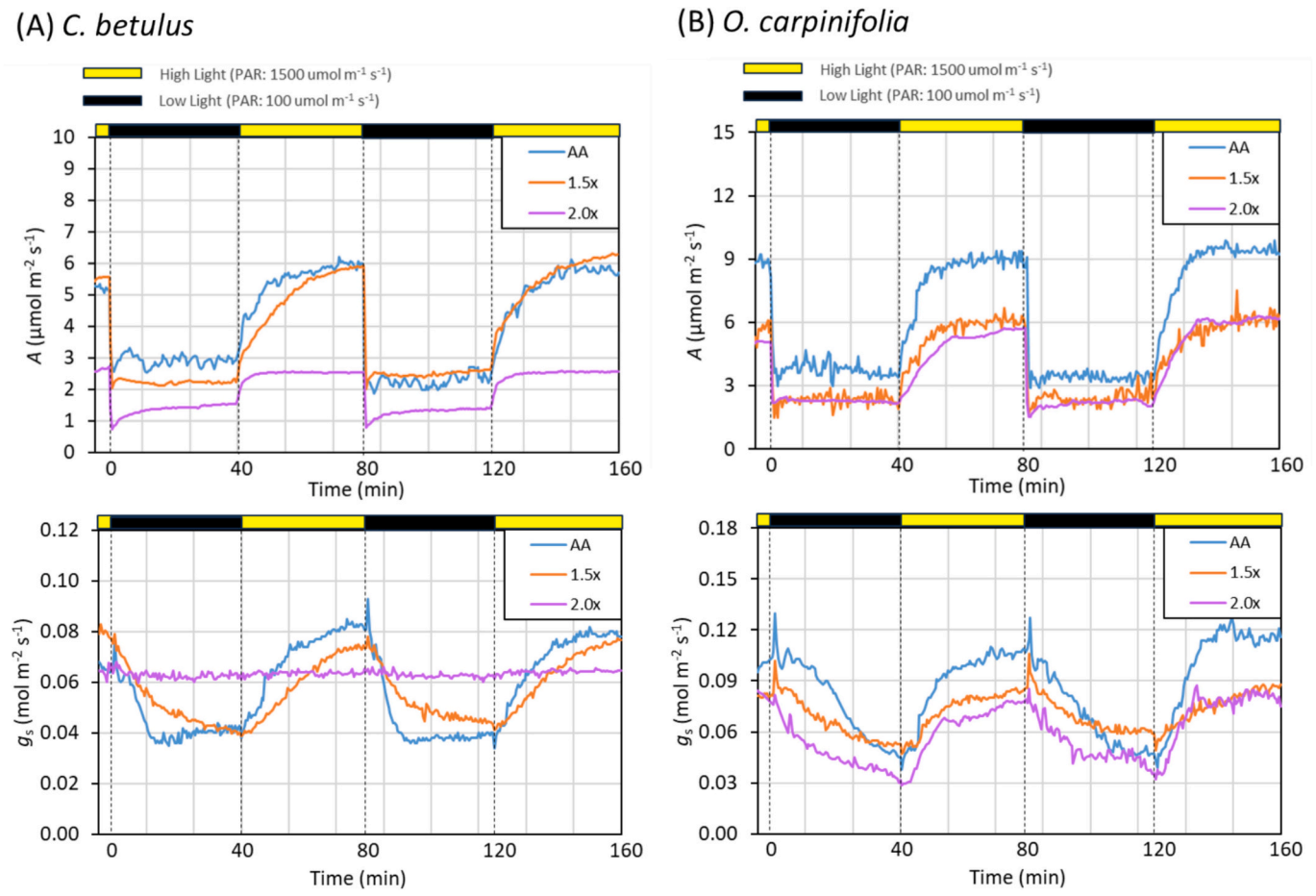

Fig. 1. Example of dynamic response of net photosynthetic rate (A) and stomatal conductance (gs) to changes in light intensity (yellow horizontal bars: PAR = 1500 μmol m^{-2} s^{-1}; black horizontal bars: PAR = 100 μmol m^{-2} s^{-1}) for *C. betulus* (CB) and *O. carpinifolia* (OC) plants exposed to three levels of O_3 (ambient air, AA; 1.5 times ambient ozone concentration, 1.5 × AA; twice ambient ozone concentration, 2.0 × AA).

further increased O_3 uptake and unexpected water loss compared to control plants (AA) with the rapid stomatal closing.

Underlying mechanisms of stomatal sluggishness are still under investigation. The slower stomatal response could potentially be attributed to the delignification of guard and subsidiary cells, as observed in O_3-exposed *Picea abies* leaves (Maier-Maercker, 1989). However, Paoletti et al. (2009) found no changes in guard cell wall lignification in O_3-damaged *Fraxinus ornus* leaves, despite exhibiting stomatal sluggishness. As stated in Uzunova (1999), CB may be a species with relatively high stomatal density. Bennett et al. (1992) suggested that species with high stomatal density may avoid injury due to their potentially faster stomatal response and lower O_3 load per single stoma. However, CB showed stomatal sluggishness rather than OC plants with lower stomatal density, which was in agreement with the findings in

Table 3
Effects of ozone exposure on dynamic response of leaf gas exchange to changes of light intensity in *Carpinus betulus* (CB) and *Ostrya carpinifolia* (OC) grown under three levels of ozone. The values (mean ± S.E.) were calculated based on the values of the measured individuals ($n = 4$ to 6 plants [1 to 2 plants per each plot per each O_3 treatment]). Asterisks show the significance of ANOVA: $^{**}p < 0.01$, $^{*}p < 0.05$, ns: not significant. When finding the interaction of O_3 and species, a Tukey post-hoc test was applied. NV: ambient air, AA; 1.5 times ambient ozone concentration, 1.5×; twice ambient ozone concentration, 2.0×). Δg_s: amplitude of gs when changing light intensity; $T90_{open}$ and $T90_{close}$: time to reach 90 % of the maximum change in stomatal opening and closure, respectively; $SLmax_{open}$ and $SLmax_{close}$: the maximum rate of change of stomatal conductance in opening and closing stomata, respectively.

Species	Ozone	Δgs (mol m^{-2} s^{-1})	$T90_{open}$ (sec)	$T90_{close}$ (sec)	$SLmax_{open}$ (μmol m^{-2} s^{-2})	$SLmax_{close}$ (μmol m^{-2} s^{-2})
CB	AA	0.063 ± 0.016	1600 ± 180	870 ± 130	64 ± 20	91 ± 14
	1.5 × AA	0.038 ± 0.015	1940 ± 150	1710 ± 280	35 ± 3	40 ± 9
	2.0 × AA	0.020 ± 0.011	2080 ± 170	1690 ± 370	16 ± 10	19 ± 9
OC	AA	0.053 ± 0.008	1500 ± 210	1400 ± 70	53 ± 22	39 ± 6
	1.5 × AA	0.024 ± 0.003	1570 ± 280	1420 ± 410	29 ± 6	28 ± 12
	2.0 × AA	0.035 ± 0.010	1160 ± 320	1800 ± 230	56 ± 28	29 ± 13
ANOVA results						
	O_3	ns	ns	ns	ns	*
	Species	ns	*	ns	ns	ns
	O_3 × Species	ns	ns	ns	ns	ns

three Chinese deciduous tree species (Hoshika et al., 2014) where O_3-induced stomatal sluggishness did not depend on stomatal density. The sluggish response of stomata may be related not only to anatomical but also physiological and/or biochemical factors. Dumont et al. (2014) found that the expression of genes involved in CO_2 signaling that triggers stomatal closure was suppressed by O_3. Recently, several studies reported that such an impairment of stomatal closing response may be related to an O_3-induced ethylene emission (Wilkinson and Davies, 2010; Hoshika et al., 2019). Considering the fact that ethylene is a phytohormone relating to senescence processes (Iqbal et al., 2017), stomatal sluggishness may be a response of O_3-induced accelerated leaf senescence. In fact, plants exposed to O_3 often show an enhanced leaf turnover, i.e. replacing damaged leaves with new leaves (Pell et al., 1994; Kitao et al., 2015). The sluggish response of stomata leads to maintaining the transpirational water flow, which may be required for an uptake of nutrients such as nitrogen for the new leaf development. However, further verification of this hypothesis is required.

Only a few studies examined the effects of O_3 on CB plants (Günthardt-Goerg et al., 1999; Marzuoli et al., 2018), and no study is available for the O_3 impacts on OC plants. Although CB might be classified as a less sensitive species to O_3 in terms of visible foliar injury (Günthardt-Goerg et al., 1999), Marzuoli et al. (2018) suggested that CB is rather sensitive to O_3 stress when nutrient availability in soils is enough for their growth, which is consistent with our result (nitrogen concentration in our soils: 1.7 g kg^{-1}, Zhang et al., 2018). Uzunova (1999) examined the leaf epidermis structure of the sub-family Coryloideae including OC and CB. This study highlighted that in OC leaves the lower epidermis, where gas exchange occurs, presents dense cuticular striations while CB shows a very thin cuticle covered with rare waxes. Furthermore, OC is equipped with trichomes unlike CB leaves where these anatomical structures are very scarce. These different structural leaf features can explain why CB is more sensitive to O_3 rather than OC, especially in terms of physiological responses. Indeed, species with thick and dense leaves and relatively high Leaf Mass per Area (LMA) demonstrated to be more resistant to O_3 damage (Manzini et al., 2023), maybe thanks to a greater antioxidant level of defense (Li et al., 2016). Moreover, the presence of trichomes in OC can increase the reaction surface with O_3 allowing its degradation and avoiding its entry inside the leaf (Oksanen, 2018). Although O_3 can also cause structural deterioration of the leaf waxes (Bytnerowicz and Turunen, 1994), the near absence of a protective waxy layer in the CB could facilitate O_3 entry. Trichomes not only act as physical barriers, but can release volatile defense compounds that can react with O_3, reducing its concentration and flux into leaves (Wedow et al., 2021; Guo et al., 2023). Conversely, the lower LMA shown by CB and lack of trichome defense may not allow for detoxifying O_3 leading to a stronger phytotoxic effect, impairment of stomatal function and photosynthesis decrease.

The linear correlation between the product of the attenuation of the terahertz radiation and L_A with W_M confirms the observation that the THz attenuation is directly proportional to the water mass. In principle, the product of the attenuation of the terahertz radiation and L_A is expected to be directly correlated with the optical thickness travelled by the radiation, that is the average thickness of the water layer contained in the leaf. Although this result is quite well established in the literature, it has been proven with different experimental setups at higher frequencies (Gente and Koch, 2015; Baldacci et al., 2017; Pagano et al., 2019); indeed, this is the first time this linear correlation is observed in the sub-THz region with an imaging setup. It may be worth noting that this linear correlation is not affected by the ozone treatment, in fact, all the three treatments were considered together in the fitting per each species. The analysis of W_M as a function of O_3 exposure indicates a reduction of W_M with the ozone treatment level. This can be explained by a higher water consumption from leaves due to the loss of closing response of stomata after O_3 exposure in these species. The result was also supported by previous findings for European silver birch (Pääkkönen et al., 1993) and hybrid poplars (Reich and Lassoie, 1984) where low leaf water content was observed in O_3-exposed leaves. In addition, the reduced leaf water content may be related to the impairment of root function under O_3 polluted environments (Andersen, 2003). In fact, O_3 may reduce the allocation to roots, which reduces the root function and thus root water uptake (Grantz et al., 1999; Agathokleous et al., 2016). Consistent with these findings, our results highlighted the impact of ozone treatment on leaves in terms of water content and its physiological responses. Interestingly, the detailed analysis of the spatial pattern of relative dry leaf area also indicates a different ability of OC and CB in treating the ozone damage. OC shows a significantly higher relative dry area at 2.0 × AA compared to AA, while CB plants have shown a relatively high dry area regardless of the O_3 treatments. In OC, the effect of O_3 on stomatal response was minor and O_3 foliar injury was not visibly well-identified. However, the negative effect of O_3 on water status was invisibly progressing with a higher relative dry area, as shown by THz radiation, which may be an early stage of the O_3 induced damages in leaf tissues and eventual cell death (Vainonen and Kangasjärvi, 2015). Since plants may show a recovery from O_3 damage (Watanabe et al., 2014), physiological acclimation response to O_3 is rather dynamic and not irreversible. Therefore, seasonal monitoring of O_3 exposed plants using the THz will be a next step.

5. Conclusions

This study explores the effect of ozone exposure on photosynthesis and leaf water status for two Hornbeams through a dual approach, utilizing Terahertz (THz) imaging and analysis of dynamic stomatal

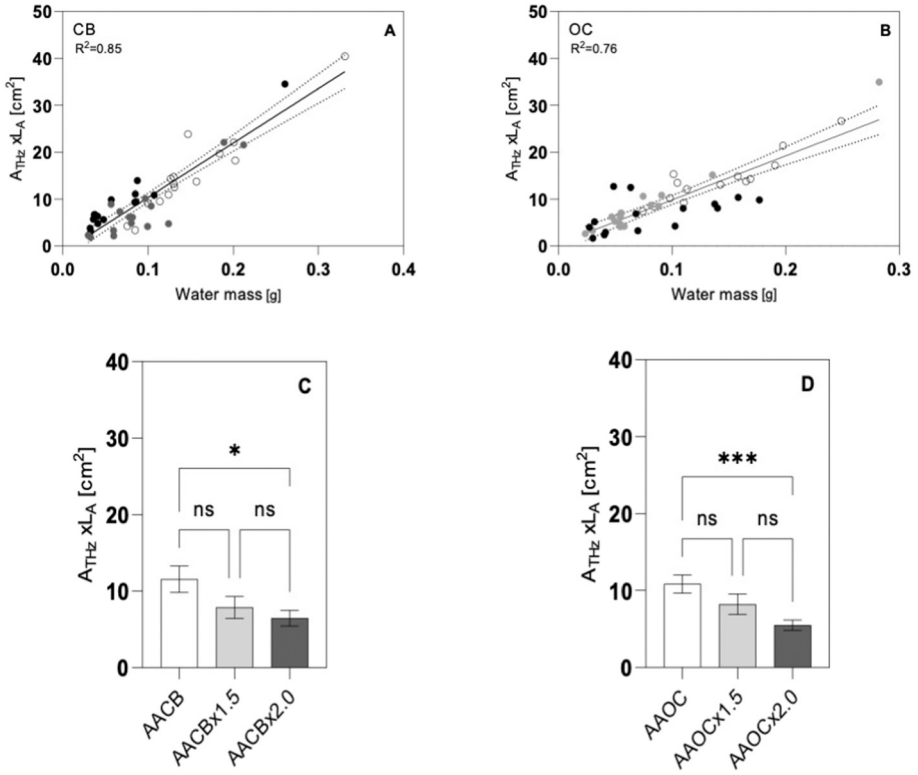

Fig. 2. The A and B graphs represent the calibration of THz acquisition versus absolute leaf water mass, with a sample size of 45 leaves and a 95 % confidence interval in *Carpinus betulus* (CB) and *Ostrya carpinifolia* (OC) grown under three levels of ozone. C and D display the results of the ANOVA analysis comparing measurements obtained through THz x L_A, based on a sample size of 25 leaves per treatment with standard errors indicated. Asterisks denote the significance of ANOVA: ***$p < 0.001$, *$p < 0.05$, ns: not significant.

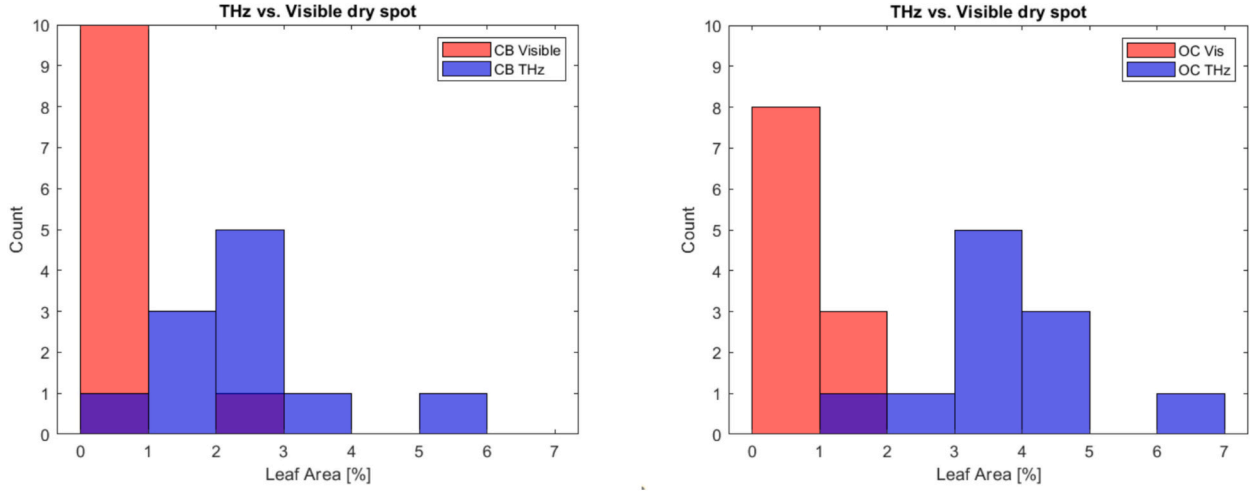

Fig. 3. Percentages of dry spot areas over the total area of the leaf in twice AA measured by visible images (Vis) and Terahertz images (THz) in *Carpinus betulus* (CB) and *Ostrya carpinifolia* (OC).

response. Stomatal sluggishness occurred especially in CB rather than OC in association with a reduction of photosynthetic capacity, suggesting that CB was more sensitive to O_3 compared to OC. This may induce unexpected water consumption for this species, and possibly cause a reduction of drought tolerance. THz-based imaging techniques, which are extremely effective for obtaining valuable in vivo data non-invasively and in real time, highlight potential implications for precision biosensing in the early detection of O_3-induced oxidative damage to plants as we detected the invisible dry spots on leaves even in the less sensitive OC plants. A novel framework for this study is the demonstration of a significant relationship between increased O_3 concentrations and decreased capacity for water regulation due to stomatal sluggishness, suggesting an implication for plant water use under climate change and O_3 pollution. The investigation provides valuable contributions to the wider discussion on plant-environment interactions, underscoring the necessity of employing multimodal approaches to unravel the complexities of O_3 -induced physiological alterations in woody plant species.

Supplementary data to this article can be found online at https://doi.org/10.1016/j.scitotenv.2024.177358.

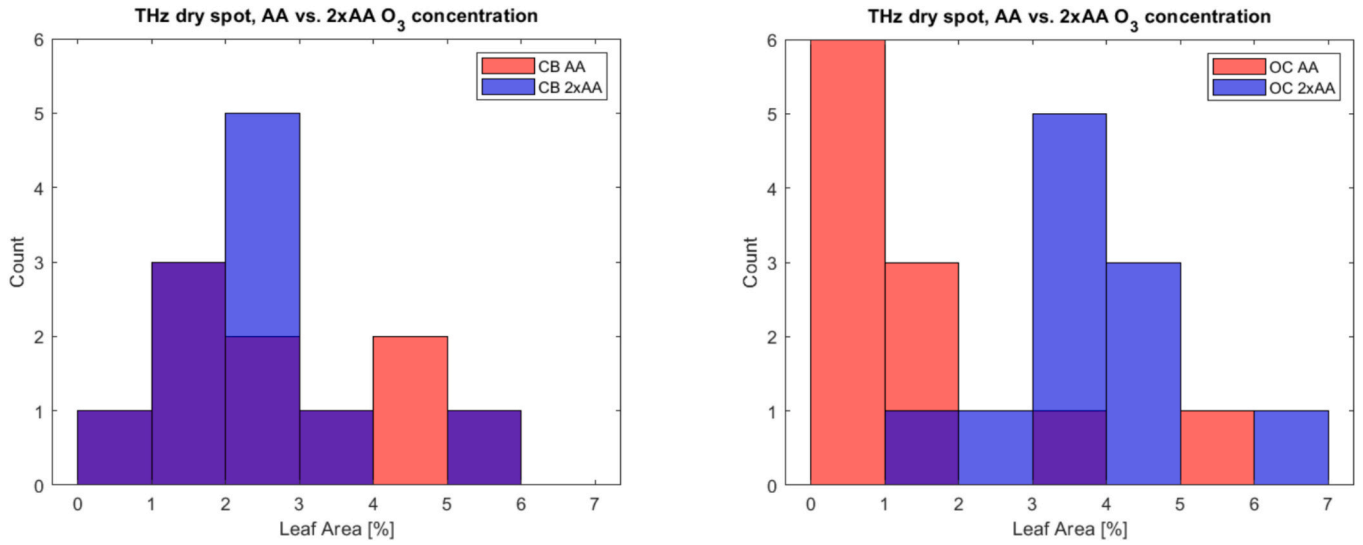

Fig. 4. Percentage of dry spot area over total area of the leaf at two ozone levels: AA and 2.0 × AA, as measured by a THz device in *Carpinus betulus* (CB) and *Ostrya carpinifolia* (OC).

CRediT authorship contribution statement

Mario Pagano: Writing – review & editing, Writing – original draft, Supervision, Methodology, Investigation, Formal analysis, Data curation. **Yasutomo Hoshika:** Writing – review & editing, Writing – original draft, Methodology, Investigation, Funding acquisition, Formal analysis, Data curation, Conceptualization. **Fulvia Gennari:** Writing – review & editing, Writing – original draft, Methodology, Investigation, Formal analysis, Data curation. **Jacopo Manzini:** Writing – review & editing, Investigation, Data curation. **Elena Marra:** Writing – review & editing, Investigation, Data curation. **Andrea Viviano:** Writing – review & editing, Investigation, Data curation. **Elena Paoletti:** Writing – review & editing, Supervision, Methodology, Investigation, Funding acquisition, Conceptualization. **Sharmin Sultana:** Writing – review & editing, Writing – original draft, Investigation, Formal analysis, Data curation. **Alessandro Tredicucci:** Writing – review & editing, Supervision, Resources, Conceptualization. **Alessandra Toncelli:** Writing – review & editing, Writing – original draft, Supervision, Methodology, Investigation, Conceptualization.

Declaration of competing interest

All the authors declare that none of the work reported in this study could have been influenced by any known competing financial interests or personal relationships.

Acknowledgements

We thank Leonardo Lazzara, Alessandro Materassi and Moreno Lazzara for the technical support, and Chiara Di Fano for the support to leaf gas exchange measurements. We thank for financial support the Fondazione Cassa di Risparmio di Firenze (2013/7956), LIFE project AIRFRESH (LIFE19 ENV/FR/000086) of the European Commission, @CNR project 4ClimAir (SAC.AD002.173.019), PNRR for Mission 4 (Component 2, Notice 3264/2021, IR0000032) – ITINERIS – Italian Integrated Environmental Research Infrastructure System CUP B53C22002150006, and National Recovery and Resilience Plan (NRRP), Mission 4 Component 2 Investment 1.4 – Call for tender No. 3138 of 16 December 2021, rectified by Decree n.3175 of 18 December 2021 of Italian Ministry of University and Research funded by the European Union – NextGenerationEU, Award Number: Project code CN_00000033, Concession Decree No. 1034 of 17 June 2022 adopted by the Italian Ministry of University and Research, CUP B83C22002930006, Project title "National Biodiversity Future Center – NBFC" (Spoke 5), Agritech National Research Center and received funding from the European Union NextGeneration EU (National Recovery and Resilience Plan (NRRP), "National Research Centre for Agricultural Tecnologies (Agritech)" – CUP I53C22000700007– Spoke n. 9).

Data availability

Data will be made available on request.

References

Agathokleous, E., Saitanis, C.J., Wang, X., Watanabe, M., Koike, T., 2016. A review study on past 40 years of research on effects of tropospheric O3 on belowground structure, functioning, and processes of trees: a linkage with potential ecological implications. Water, Air, Soil Poll. 227, 1–28. https://doi.org/10.1007/s11270-015-2715-9.

Agathokleous, E., Kitao, M., Hoshika, Y., Haworth, M., Tang, Y., Koike, T., 2023. Ethylenediurea protects against ozone phytotoxicity not by adding nitrogen or controlling stomata in a stomata-unresponsive hybrid poplar. Sci. Tot. Environ. 875, 162672. https://doi.org/10.1016/j.scitotenv.2023.162672.

Agrawal, S.B., Agrawal, M., Singh, A. (Eds.), 2021. Tropospheric Ozone: A Hazard for Vegetation and Human Health. Cambridge Scholars Publishing., ISBN (10): 1-5275-7057-6. p. 646.

Andersen, C.P., 2003. Source–sink balance and carbon allocation below ground in plants exposed to ozone. New Phytol. 157, 213–228. https://doi.org/10.1046/j.1469-8137.2003.00674.x.

Ansari et al. 2023. Ozone exposure response on physiological and biochemical parameters vis-a-vis secondary metabolites in a traditional medicinal plant *Sida cordifolia* L. DOI: https://doi.org/10.1016/j.indcrop.2023.116267.

Baldacci, L., Pagano, M., Masini, L., Toncelli, A., Carelli, G., Storchi, P., Tredicucci, A., 2017. Non-invasive absolute measurement of leaf water content using terahertz quantum cascade lasers. Plant Methods. https://doi.org/10.1186/s13007-017-0197-z.

Bastias, C.C., Truchado, D.A., Valladares, F., Benavides, R., Bouriaud, O., Bruelheide, H., Coppi, A., Finér, L., Gimeno, T.E., Jaroszewicz, B., Scherer-Lorenzen, M., Selvi, F., De la Cruz, M., 2020. Species richness influences the spatial distribution of trees in European forests. Oikos 129 (3), 380–390.

Bennett, J.P., Rassat, P., Berrang, P., Karnosky, D.F., 1992. Relationships between leaf anatomy and ozone sensitivity of *Fraxinus pennsylvanica* Marsh. and *Prunus serotina* Ehrh. Environ. Exp. Bot. 32 (1), 33–41.

Born, N., Behringer, D., Liepelt, S., Beyer, S., Schwerdtfeger, M., Ziegenhagen, B., Koch, M., 2014. Monitoring plant drought stress response using terahertz time-domain spectroscopy. Plant Physiol. 164, 1571–1577. https://doi.org/10.1104/pp.113.23360.

Bytnerowicz, A., Turunen, M., 1994. Effects of ozone exposures on epicuticular wax of ponderosa pine needles. In: Air Pollutants and the Leaf Cuticle. Springer Berlin Heidelberg, Berlin, Heidelberg, pp. 305–314.

Castro-Camus, E., Palomar, M., Covarrubias, A.A., 2013. Leaf water dynamics of Arabidopsis thaliana monitored in-vivo using terahertz time-domain spectroscopy. Sci. Rep. 3, 2910. https://doi.org/10.1038/srep02910.

Cotrozzi, L., Lorenzini, G., Nali, C., Pellegrini, E., Saponaro, V., Hoshika, Y., Arab, L., Rennenberg, H., Paoletti, E., 2020. Hyperspectral reflectance of light-adapted leaves can predict both dark- and light-adapted Chl fluorescence parameters, and the effects of chronic ozone exposure on date palm (Phoenix dactylifera). Int. J. Mol. Sci. 21, 6441. https://doi.org/10.3390/ijms21176441.

De Marco, A., Sicard, P., Feng, Z., Agathokleous, E., Alonso, R., Araminiene, V., Augustatis, A., Badea, O., Beasley, J.C., Branquinho, C., Bruckman, V.J., Collalti, A., David-Schwartz, R., Domingos, M., Du, E., Garcia Gomez, H., Hashimoto, S., Hoshika, Y., Jakovljevic, T., McNulty, S., Oksanen, E., Omidi Khaniabadi, Y., Prescher, A.-K., Saitanis, C.J., Sase, H., Schmitz, A., Voigt, G., Watanabe, M., Wood, M.D., Kozlov, M.V., Paoletti, E., 2022. Strategic roadmap to assess forest vulnerability under air pollution and climate change. Glo. Chan. Bio. 28, 5062–5085. https://doi.org/10.1111/gcb.16278.

Di Girolamo, F.V., Toncelli, A., Tredicucci, A., Bitossi, M., Paoletti, E., 2020. Leaf water diffusion dynamics in vivo through a sub-terahertz portable imaging system. In. J. Phys. Conf. Ser. 1548, 012002. https://doi.org/10.1088/1742-6596/1548/1/012002.

Dumont, J., Cohen, D., Gérard, J., Jolivet, Y., Dizengremel, P., Le Thiec, D., 2014. Distinct responses to ozone of abaxial and adaxial stomata in three Euramerican poplar genotypes. Plant Cell Environ. 37 (9), 2064–2076.

Durand, M., Brendel, O., Buré, C., Le Thiec, D., 2019. Altered stomatal dynamics induced by changes in irradiance and vapour-pressure deficit under drought: impacts on the whole-plant transpiration efficiency of poplar genotypes. New Phytol. 222 (4), 1789–1802.

Endo, R., Omasa, K., 2007. 3-D cell-level chlorophyll fluorescence imaging of ozone-injured sunflower leaves using a new passive light microscope system. J. Exp. Bot. 58, 765–772. https://doi.org/10.1093/jxb/erl210.

Feng, Z., Xu, Y., Kobayashi, K., Dai, L., Zhang, T., Agathokleous, E., Calatayud, V., Paoletti, E., Mukherjee, A., Agrawal, M., Park, R.J., Oak, Y.J., Yue, X., 2022. Ozone pollution threatens the production of major staple crops in East Asia. Nat. Food 3, 47–56. https://doi.org/10.1038/s43016-021-00422-6.

Freitas, R.S., Oliveira, L.A., McAdam, S.A., Lawson, T., DaMatta, F.M., Cardoso, A.A., 2023. Woody species grown under sun and shade present similar stomatal speed. Theoretical Exp. Plant Physiol. 35 (3), 275–286.

Gente, R., Koch, M., 2015. Monitoring leaf water content with THz and sub-THz waves. Plant Methods 11, 1–9. https://doi.org/10.1186/s13007-015-0057-7.

Gerardin, T., Douthe, C., Flexas, J., Brendel, O., 2018. Shade and drought growth conditions strongly impact dynamic responses of stomata to variations in irradiance in Nicotiana tabacum. Environ. Exp. Bot. 153, 188–197.

Gerosa, G.A., Marzuoli, R., Finco, A., 2022. Interannual variability of ozone fluxes in a broadleaf deciduous forest in Italy. Elem. Sci. Anth. 10 (1), 00105.

Grantz, D.A., Zhang, X., Carlson, T., 1999. Observations and model simulations link stomatal inhibition to impaired hydraulic conductance following ozone exposure in cotton. Plant Cell Environ. 22, 1201–1210. https://doi.org/10.1046/j.1365-3040.1999.00486.x.

Grulke, N.E., Heath, R.L., 2020. Ozone effects on plants in natural ecosystems. Plant Bio. 22, 12–37. https://doi.org/10.1111/plb.12971.

Günthardt-Goerg, M.S., Maurer, S., Bolliger, J., Clark, A.J., Landolt, W., Bucher, J.B., 1999. Responses of young trees (five species in a chamber exposure) to near-ambient ozone concentrations. In: Sheppard, L.J., Cape, J.N. (Eds.), Forest Growth Responses to the Pollution Climate of the 21st Century. Springer, Dordrecht. https://doi.org/10.1007/978-94-017-1578-2_25.

Guo, C., Wang, X., Wang, Q., Zhao, Z., Xie, B., Xu, L., Zhang, R., 2023. Plant defense mechanisms against ozone stress: insights from secondary metabolism. Environ. Exp. Bot. 105553.

Hoshika, Y., Wanatabe, M., Inada, N., Koike, T., 2012. Ozone-induced stomatal sluggishness develops progressively in Siebold's beech (Fagus crenata). Environ. Pollut. 166, 152–156. https://doi.org/10.1016/j.envpol.2012.03.013.

Hoshika, Y., Carriero, G., Feng, Z., Zhang, Y., Paoletti, E., 2014. Determinants of stomatal sluggishness in ozone-exposed deciduous tree species. Sci. Tot. Environ. 481, 453–458.

Hoshika, Y., Katata, G., Deushi, M., Watanabe, M., Koike, T., Paoletti, E., 2015. Ozone-induced stomatal sluggishness changes carbon and water balance of temperate deciduous forests. Sci. Rep. 5, 9871. https://doi.org/10.1038/srep09871.

Hoshika, Y., De Carlo, A., Baraldi, R., Neri, L., Carrari, E., Agathokleous, E., Zhang, L., Fares, S., Paoletti, E., 2019. Ozone-induced impairment of night-time stomatal closure in O3-sensitive poplar clone is affected by nitrogen but not by phosphorus enrichment. Sci. Tot. Environ. 692, 713–722. https://doi.org/10.1016/j.scitotenv.2019.07.288.

Hoshika, Y., Fares, S., Pellegrini, E., Conte, A., Paoletti, E., 2020. Water use strategy affects avoidance of ozone stress by stomatal closure in Mediterranean trees—a modelling analysis. Plant Cell Environ. 43, 611–623. https://doi.org/10.1111/pce.13700.

Hoshika, Y., Paoletti, E., Centritto, M., Gomes, M.T.G., Puértolas, J., Haworth, M., 2022. Species-specific variation of photosynthesis and mesophyll conductance to ozone and drought in three Mediterranean oaks. Physiol. Plant. 174, e13639. https://doi.org/10.1111/ppl.13639.

IPCC, 2013. Climate Change 2013 – The Physical Science Basis. Cambridge University Press, Cambridge, 1552 pp. https://www.ipcc.ch/site/assets/uploads/2018/04/press_release_wg1_full_report.pdf.

Iqbal, N., Khan, N.A., Ferrante, A., Trivellini, A., Francini, A., Khan, M.I.R., 2017. Ethylene role in plant growth, development and senescence: interaction with other phytohormones. Front. Plant Sci. 8, 475. https://doi.org/10.3389/fpls.2017.00475.

Kattge, J., Knorr, W., Raddatz, T., Wirth, C., 2009. Quantifying photosynthetic capacity and its relationship to leaf nitrogen content for global-scale terrestrial biosphere models. Glob. Chan. Bio. 15, 976–991. https://doi.org/10.1111/j.1365-2486.2008.01744.x.

Kitao, M., Löw, M., Heerdt, C., Grams, T.E., Häberle, K.H., Matyssek, R., 2009. Effects of chronic elevated ozone exposure on gas exchange responses of adult beech trees (Fagus sylvatica) as related to the within-canopy light gradient. Environ. Pol. 157, 537–544. https://doi.org/10.1016/j.envpol.2008.09.016.

Kitao, M., Komatsu, M., Yazaki, K., Kitaoka, S., Tobita, H., 2015. Growth overcompensation against O3 exposure in two Japanese oak species, Quercus mongolica var. crispula and Quercus serrata, grown under elevated CO2. Environ. Pol. 206, 133–141. https://doi.org/10.1016/j.envpol.2015.06.034.

Koike, T., Watanabe, T., Toda, H., Haibara, K., 1998. Morphological diversity of stomata of representative broadleaved trees in a temperate region: detection with the Sump method. For. Resources Environ. 36, 55–63.

Larcher, W., 2003. Physiological Plant Ecology, 4th ed. Springer-Verlag, New York. https://doi.org/10.1086/419487.

Li, P., Calatayud, V., Gao, F., Uddling, J., Feng, Z., 2016. Differences in ozone sensitivity among woody species are related to leaf morphology and antioxidant levels. Tree Phys. 36, 1105–1116. https://doi.org/10.1093/treephys/tpw042.

Li, P., Feng, Z., Catalayud, V., Yuan, X., Xu, Y., Paoletti, E., 2017. A meta-analysis on growth, physiological, and biochemical responses of woody species to ground-level ozone highlights the role of plant functional types. Plant Cell Environ. 40, 2369–2380. https://doi.org/10.1111/pce.13043.

Lombardozzi, D., Sparks, J.P., Bonan, G., Levis, S., 2012. Ozone exposure causes a decoupling of conductance and photosynthesis: implications for the ball-berry stomatal conductance model. Oecologia 169, 651–659. https://doi.org/10.1007/s00442-011-2242-3.

Maier-Maercker, U., 1989. Delignification of subsidiary and guard cell walls of *Picea abies* (L.) Karst. by fumigation with ozone. Trees 3, 57–64.

Manes, F., Vitale, M., Donato, E., Paoletti, E., 1998. O3 and O3+ CO2 effects on a Mediterranean evergreen broadleaf tree, holm oak (Quercus ilex L.). Chemosphere 36, 801–806. https://doi.org/10.1016/S0045-6535(97)10127-8.

Manzini, J., Hoshika, Y., Moura, B.B., Paoletti, E., 2023. Exploring a new O3 index as a proxy for the avoidance/tolerance capacity of forest species to tolerate O3 injury. Forests 14, 901. https://doi.org/10.3390/f14050901.

Marchica, A., Pellegrini, E., 2023. The intriguous roles of phytohormones in plant response to ozone interacting with other major climate change stressors. In: Ahammed, G.J., Yu, J. (Eds.), Plant Hormones and Climate Change. Springer, Singapore. https://doi.org/10.1007/978-981-19-4941-8_4.

Marzuoli, R., Monga, R., Finco, A., Chiesa, M., Gerosa, G., 2018. Increased nitrogen wet deposition triggers negative effects of ozone on the biomass production of Carpinus betulus L. young trees. Environ. Experim. Botany 152, 128–136. https://doi.org/10.1016/j.envexpbot.2017.10.017.

McLaughlin, S.B., Nosal, M., Wullschleger, S.D., Sun, G., 2007. Interactive effects of ozone and climate on tree growth and water use in a southern Appalachian Forest in the USA. New Phytol. 174, 109–124. https://doi.org/10.1111/j.1469-8137.2007.02018.x.

Mochizuki, T., Ikeda, F., Tani, A., 2020. Effect of growth temperature on monoterpene emission rates of Acer palmatum. Sci. Tot. Environ. 745, 140886. https://doi.org/10.1016/j.scitotenv.2020.140886.

Oksanen, E., 2018. Trichomes form an important first line of defence against adverse environment—new evidence for ozone stress mitigation. Plant Cell Environ. 41, 1497–1499. https://doi.org/10.1111/pce.13187.

Pääkkönen, E., Paasisalo, S., Holopainen, T., Kärenlamp, L., 1993. Growth and stomatal responses of birch (Betula pendula Roth.) clones to ozone in open-air and chamber fumigations. New Phytol. 125, 615–623. https://doi.org/10.1111/j.1469-8137.1993.tb03911.x.

Pagano, M., Baldacci, L., Ottomaniello, A., De Dato, G., Chianucci, F., Masini, L., Carelli, G., Toncelli, A., Storchi, P., Tredicucci, A., Corona, P., 2019. THz water transmittance and leaf surface area: an effective nondestructive method for determining leaf water content. Sensors 19, 4838. https://doi.org/10.3390/s19224838.

Paoletti, E., 2005. Ozone slows stomatal response to light and leaf wounding in a Mediterranean evergreen broadleaf, Arbutus unedo. Environ. Pol. 134, 439–445. https://doi.org/10.1016/j.envpol.2004.09.011.

Paoletti, E., Contran, N., Bernasconi, P., Günthardt-Goerg, M.S., Vollenweider, P., 2009. Structural and physiological responses to ozone in Manna ash (*Fraxinus ornus* L.) leaves of seedlings and mature trees under controlled and ambient conditions. Sci. Tot. Environ. 407 (5), 1631–1643.

Paoletti, E., Grulke, N., 2010. Ozone exposure and stomatal sluggishness in different plant physiological classes. Environ. Pollut. 158, 2664–2671. https://doi.org/10.1016/j.envpol.2010.04.024.

Paoletti, E., Materassi, A., Fasano, G., Hoshika, Y., Carriero, G., Silaghi, D., Badea, O., 2017. A new-generation 3D ozone FACE (free air controlled exposure). Sci. Tot. Environ. 575, 1407–1414. https://doi.org/10.1016/j.scitotenv.2016.09.217.

Pasta, S., de Rigo, D., Caudullo, G., 2016. *Ostrya carpinifolia* in Europe: distribution, habitat, usage and threats. In: San-MiguelAyanz, J., de Rigo, D., Caudullo, G., Houston Durrant, T., Mauri, A. (Eds.), European Atlas of Forest Tree Species. Publ. Off. EU, Luxembourg, pp. e01fd3d+.

Pell, E.J., Temple, P.J., Friend, A.L., Mooney, H.A., Winner, W.E., 1994. Compensation as a plant response to ozone and associated stresses: an analysis of ROPIS experiments. J. Environ. Qual. 23, 429–436. https://doi.org/10.2134/jeq1994.00472425002300030005x.

Peng et al. 2020. Effects of ozone on maize (*Zea mays* L.) photosynthetic physiology, biomass and yield components based on exposure- and flux-response relationships DOI: https://doi.org/10.1016/j.envpol.2019.113466.
Rawson, A., Sunil, C.K., 2022. Recent advances in terahertz time-domain spectroscopy and imaging techniques for automation in agriculture and food sector. Food Anal. Methods 15, 498–526. https://doi.org/10.1007/s12161-021-02132-y.
Reich, P.B., Lassoie, J.P., 1984. Effects of low level O3 exposure on leaf diffusive conductance and water-use efficiency in hybrid poplar. Plant Cell Environ. 7, 661–668. https://doi.org/10.1111/1365-3040.ep11571645.
Sikkema, R., Caudullo, G., de Rigo, D., 2016. Carpinus betulus in Europe: distribution, habitat, usage and threats. In: San-MiguelAyanz, J., de Rigo, D., Caudullo, G., Houston Durrant, T., Mauri, A. (Eds.), European Atlas of Forest Tree Species. Publ. Off. EU, Luxembourg, pp. e01d8cf+.
Sun, G.E., McLaughlin, S.B., Porter, J.H., Uddling, J., Mulholland, P.J., Adams, M.B., Pederson, N., 2012. Interactive influences of ozone and climate on streamflow of forested watersheds. Glob. Chang. Biol. 18, 3395–3409. https://doi.org/10.1111/j.1365-2486.2012.02787.x.
Tinoco-Ojanguren, C., Pearcy, R.W., 1993. Stomatal dynamics and its importance to carbon gain in two rainforest Piper species. Oecologia 94, 388–394. https://doi.org/10.1007/BF00317115.
Tjoelker, M.G., Volin, J.C., Oleksyn, J., Reich, P.B., 1995. Interaction of ozone pollution and light effects on photosynthesis in a forest canopy experiment. Plant Cell Environ. 18 (8), 895–905.
Tomimatsu, H., Tang, Y., 2012. Elevated CO2 differentially affects photosynthetic induction response in two Populus species with different stomatal behavior. Oecologia 169, 869–878. https://doi.org/10.1007/s00442-012-2256-5.
Torres, V., Palacios, I., Iriarte, J.C., Liberal, I., Santesteban, L.G., Miranda, C., Royo, J.B., Gonzalo, R., 2016. Monitoring water status of grapevine by means of THz waves. J. Infrared Milli. Terah. Waves 37, 507–513. https://doi.org/10.1007/s10762-016-0269-6.
Uzunova, K.R., 1999. A comparative study of leaf epidermis in European Corylaceae. Feddes Repert. 110, 209–218. https://doi.org/10.1002/fedr.19991100307.
Vainonen, J.P., Kangasjärvi, J., 2015. Plant signalling in acute ozone exposure. Plant Cell Environ. 38 (2), 240–252.
VanLoocke, A., Betzelberger, A.M., Ainsworth, E.A., Bernacchi, C.J., 2012. Rising ozone concentrations decrease soybean evapotranspiration and water use efficiency whilst increasing canopy temperature. New Phytol. 195, 164–171. https://doi.org/10.1111/j.1469-8137.2012.04152.x.
Vialet-Chabrand, S., Dreyer, E., Brendel, O., 2013. Performance of a new dynamic model for predicting diurnal time courses of stomatal conductance at the leaf level. Plant Cell Environ. 36, 1529–1546.
Wada, R., Yonemura, S., Tani, A., Kajino, M., 2023. Exchanges of O3, NO, and NO2 between forest ecosystems and the atmosphere. J. Agricult. Meteor. 79, 38–48. https://doi.org/10.2480/agrmet.D-22-00023.
Watanabe, M., Hoshika, Y., Koike, T., 2014. Photosynthetic responses of monarch birch seedlings to different timing of free air ozone fumigation. J. Plant Res. 127, 339–345. https://doi.org/10.1007/s10265-013-0622-y.
Wedow, J.M., Ainsworth, E.A., Li, S., 2021. Plant biochemistry influences tropospheric ozone formation, destruction, deposition, and response. Trends Biochem. Sci. 46 (12), 992–1002.
Wilkinson, S., Davies, W.J., 2010. Drought, ozone, ABA and ethylene: new insights from cell to plant to community. Plant Cell Environ. 33, 510–525. https://doi.org/10.1111/j.1365-3040.2009.02052.x.
Wittig, V.E., Ainsworth, E.A., Long, S.P., 2007. To what extent do current and projected increases in surface ozone affect photosynthesis and stomatal conductance of trees? A meta-analytic review of the last 3 decades of experiments. Plant Cell Environ. 30, 1150–1162. https://doi.org/10.1111/j.1365-3040.2007.01717.x.
Zhang, L., Hoshika, Y., Carrari, E., Badea, O., Paoletti, E., 2018. Ozone risk assessment is affected by nutrient availability: evidence from a simulation experiment under free air controlled exposure (FACE). Environ. Pol. 238, 812–822. https://doi.org/10.1016/j.envpol.2018.03.102.
Zhang, X., Wang, X., Wang, Y., Hu, L., Wang, P., 2023. Detection of tomato water stress based on terahertz spectroscopy. Front. Plant Scien. 14, 1095434. https://doi.org/10.3389/fpls.2023.1095434.